NUMERICAL INVESTIGATION OF CRACK ORIENTATION IN THE FRETTING FATIGUE OF A FLAT ROUNDED CONTACT

A. Mohajerani

Department of Mechanical and Industrial Engineering, University of Toronto, 5 King's College Road, Toronto, ON, Canada M5S 3G8

G.H. Farrahi*

[b]*School of Mechanical Engineering, Sharif University of Technology, Azadi Ave., Tehran, Iran*
Email: farrahi@sharif.edu

*Corresponding Author

(Received: February 16, 2010 – Accepted in Revised Form: November 11, 2010)

Abstract The growth of slant cracks by fretting fatigue of a half plane in contact with a flat rounded pad was studied. The mode I and mode II stress intensity factors for cracks of various lengths and directions were calculated using the semi-analytical method of the distribution of dislocations, and their cumulative effect on the crack growth was investigated using the strain energy density criterion. The results showed dominance of mode I fracture on crack growth, and based on the observation of strain energy density factor versus crack orientation, the results also suggest that depending on the crack length, the most critical orientations of cracks are at 0^0 to 20^0 outward the contact zone. Good agreement was observed between the results of this semi-analytical approach, and the corresponding results from finite element method, for selected crack lengths and orientations.

Keywords Fretting fatigue, Contact mechanics, Slant crack, Distribution of dislocations.

چکیده رشد ترک های ناشی از اریب خستگی سایشی یک نیم صفحه در تماس با یک کفشک مسطح لبه گرد مورد مطالعه قرار گرفت. ضرایب شدت تنش مدهای ۱ و ۲ برای ترک هایی با طول و جهات مختلف، با بکارگیری روش نیمه تحلیلی " توزیع نابجایی ها" محاسبه گردیدند و همچنین تاثیر تجمیعی آنها بر روی رشد ترک با استفاده از معیار انرژی کرنشی، مورد بررسی قرار گرفت. نتایج، برتری شکست مد ۱ را در رشد ترک نشان داد. همچنین نتایج مبنی بر مشاهدات تغییرات چگالی انرژی کرنشی در رابطه با جهت رشد ترک نشان می دهند، که بسته به طول ترک، بحرانی ترین جهت ترک ۰ تا ۲۰ درجه به سمت منطقه تماس می باشد. ضمنا توافق خوبی بین نتایج روش نیمه تحلیلی و نتایج اجزاء محدود برای ترک های با طول وجهت مختلف مشاهده شد.

1. INTRODUCTION

Fretting fatigue induces damage at or near the contact surfaces and results in the reduction of fatigue life compared to the normal fatigue with no contacting components. Fretting is caused by micro-slip of the contact surfaces and the formation of highly stressed zones near the contact surfaces. This damage is widespread in the dovetail regions of aero engine compressor disks which experience fretting in a flat-on-flat contact with a relatively large radius at the edge of the contact [1-4]. Since experimental setups are costly and stress states are mostly unknown, simplified models of the dovetail region are widely used for analysis purposes. One such model is that of a flat and rounded pad in contact with a half plane placed under the fretting loading. This model is favorable because of its similarity to the mechanism of contact in the dovetail region and also its analytical simplicity [2, 5-12].

Fretting cracks generally undergo mixed loading, and a proper study on them requires the consideration of crack growth under mixed modes fracture patterns. Several studies have shown that there is much tendency for the short fretting cracks to grow in an oblique manner rather than simply normal to the contact surfaces [13-17].

In the present work, the growth of slant fretting cracks from a fracture mechanics point of view was studied. Fretting fatigue of a half plane in contact with a flat rounded pad placed under fretting loading was taken into consideration. The stress intensity factors (SIF) of resulting slant fretting cracks in the first and second modes were calculated and their cumulative effect on crack growth was investigated using the strain energy density criterion. Cracks were assumed to appear at the contact boundary and various lengths and angles are considered for them. A semi-analytical method of the distribution of dislocations was applied for the calculation of SIFs and a good agreement was observed with finite element method results.

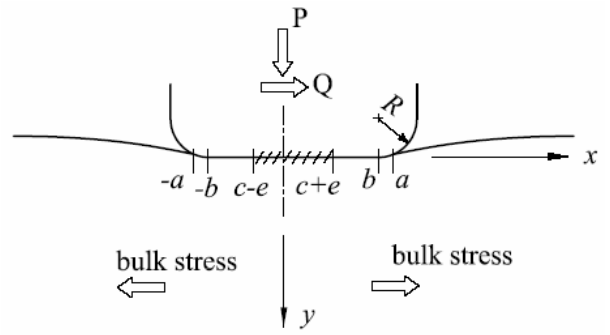

Figure 1. A schematic illustration of a flat and rounded contact configuration

Distribution of dislocations method is based on the numerical calculation of integral equations which relates the stress state of the uncracked half plane and relative displacement of crack faces, so that the first step in its application is to calculate the stress state of the uncracked half plane [16]. Results of the study show the most and least critical angles of slants cracks and their variations with respect to the crack length.

2. STRESS STATE IN THE HALF PLANE

2.1. Normal and shear tractions calculation In this section, we describe the method employed to calculate stress state with respect to a typical geometry of the pad. Figure 1 shows the configuration of the contact model. The contact area has a width of 2*a* and a stick zone width of 2*c*. The pad has a flat central part of width 2*b* and two rounded corners of radius R. These corners are approximated by parabolic curves. The half plane is subjected to not only the normal force, P, and tangential force, Q, but also to a bulk stress, σ_b. As the result of bulk stress introduction to the half plane, the stick zone shifts by a value of *e*, and the shear traction distribution becomes asymmetrical. Although the presence of bulk stress results in more complications in analytical solutions, it is necessary to be taken into account as the fretting fatigue which normally takes place in the presence of bulk stresses within one or both of the contacting bodies caused by loading other than contact itself.

For the case that flat rounded pad and half plane have the same modulus of elasticity, *E*, and Poisson's ratio, *v*, the equation used for calculation of the normal traction, *p(x)*, can be written as [17]:

$$\pi AR\,p(x) = x\ln\frac{\left(b\sqrt{a^2-x^2}+x\sqrt{a^2-b^2}\right)^2}{a^2\left|x^2-b^2\right|} - b\ln\frac{\left(\sqrt{a^2-b^2}+\sqrt{a^2-x^2}\right)^2}{\left|x^2-b^2\right|}+2\sqrt{a^2-x^2}\arccos\frac{b}{a} \quad (1)$$

where, *A* is given by

$$A=\frac{\kappa+1}{2G} \qquad \kappa=\begin{cases}3-4v & \text{for plane strain}\\ \dfrac{3-v}{1+v} & \text{for plane stress}\end{cases} \quad (2)$$

G is the modulus of rigidity. In this paper we only consider the case of moderate bulk stress, for which tangential traction has the same sign over the entire contact area. Using the relation between shear traction, *q(x)*, and the tangential relative slip of surface points, *g(x)*, we calculate the unknown *q(x)* [17]:

$$\frac{1}{A}\frac{\partial g}{\partial x}=\frac{1}{\pi}\int_{-a}^{a}\frac{q(\zeta)}{\zeta-x}d\zeta-\frac{\sigma_b}{4} \quad (3)$$

The shear traction can be defined as:

$$q(x) = q^*(x), \qquad |x-e| \le c$$
$$q(x) = f|p(x)|, \qquad a \le x \le -c+e \cup c+e \le x \le a \quad (4)$$

where f is the coefficient of friction. By substituting Eq. 4 into Eq. 3 in the stick zone we obtain [17]:

$$\frac{\sigma_b}{4} - \frac{1}{\pi}\int_{-a}^{a} \frac{f.|p(\xi)|}{\xi - x} d\xi = \int_{e-c}^{e+c} \frac{q^*(\xi)}{\xi - x} d\xi \quad (5)$$

Gauss-Chebyshev quadrature method can be used to solve Eq. 5 [18]. The same procedure used in ref. [19] is also applied here to find the shear traction in certain points. The stick zone shift and σ_b are related variables and only one of them can be chosen. The relation between the mentioned variables can be found by invoking the consistency condition [20].Through the calculation of normal and shear tractions on the contact surface, the values of normal and tangential forces can be found using the equilibrium conditions of the pad [17].

2.2. Interior stress state Stress state in the half plane is given by the superposition of the contact-induced stress state and the bulk stress. In order to evaluate the contact-induced stress state, we consider the pressure and the shear tractions as arrays of overlapping triangular traction elements. The use of such elements results in a piecewise linear approximation to the surface tractions and is thus free from discontinuities associated with the piecewise method [21]. The stress state due to each traction element is calculated and used to obtain the total contact-induced stress state. For the convenience, we use only the first component of the stress state, σ_x , for demonstration purposes in the following sections, although one should note that this method can be used to efficiently calculate all three of the σ_x, σ_y and τ_{xy} components of the stress state.

3. FINITE ELEMENT MODELING

The finite element modeling of normal cracks of different lengths were carried out using ANSYS software. The configuration of the contact model is shown is Figure 2. This model has been excessively used in the literature [5, 6, 19, 22] because of its similarity to most of the fretting fatigue experimental setups. In finite element modeling of this configuration, the lower plate should be taken large enough to appropriately approximate a half plane.

The model is loaded in two steps. In the first load step, normal force is exerted to the pad and in the second step the bulk stress, σ_b, is applied to the lower plate. Notice that the bulk stress automatically brings about the tangential force Q.

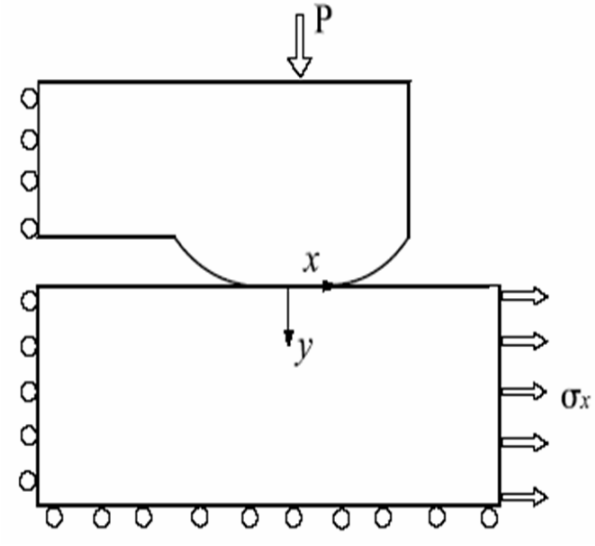

Figure 2. The configuration of the finite element model of the contact under fretting loading, and the applied loads

As shown in Figure. 3, in order to create the moment, M, necessary for the equilibrium of the pad, the pressure distribution over the contact surface should be asymmetric. However, pressure distribution in homogeneous contacts should be independent of the tangential loads, thus in the case of flat and rounded contact it has to be symmetrical. The symmetry of pressure distribution is a significant concern in the finite element modeling and can be greatly overcome by coupling the nodes of the pad's upper side in y direction.

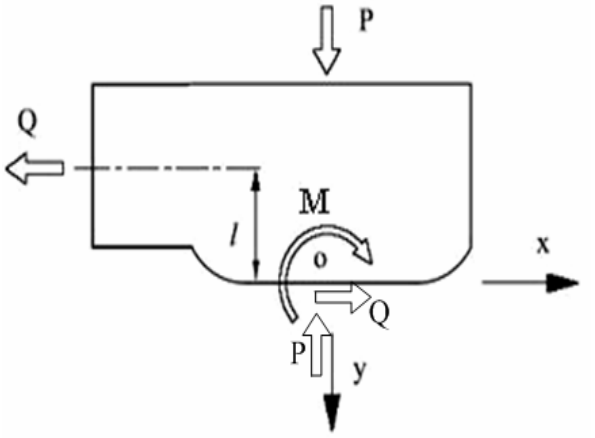

Figure 3. A schematic view of the applied loads and reactions forces on the pad.

The crack tips in the finite element model were meshed using triangular PLANE2 singular elements. These elements have triangular shape, and are defined by six nodes having two degrees of freedom at each node. These singular elements are capable of obtaining the well-established singular stress field near the crack tip by shifting the mid-side nodes one-quarter away from the crack tip. The crack tips were meshed with 12 singular elements of 0.05% of crack length, according to the results presented in [23].

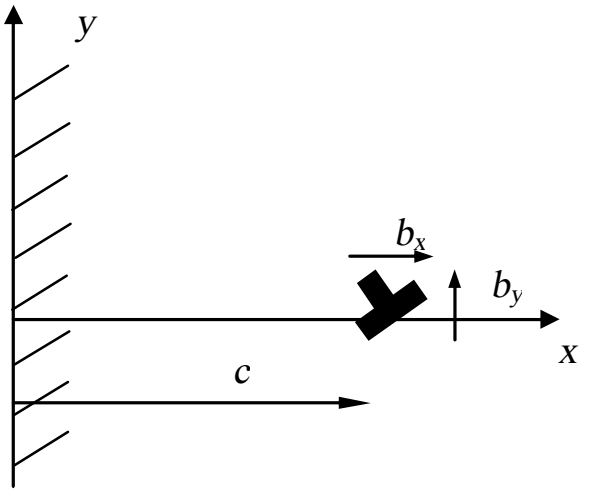

Figure 4. An arbitrarily oriented dislocation in a half plane

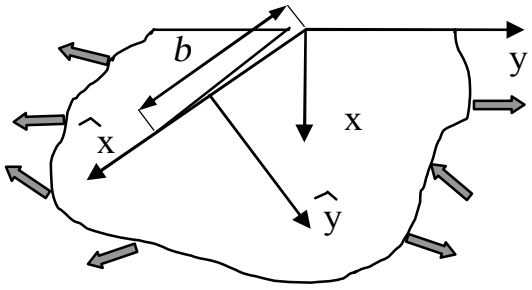

Figure 5. A half plane subjected to an arbitrary inclined crack

4. DISTRIBUTION OF DISLOCATIONS METHOD

The distribution of dislocations method is a convenient approach for calculating SIFs of cracks in the half planes under complicated stress states [5, 16, 24, 25]. This method is based on the numerical solution of integral equations which relate the relative displacement of the crack faces and the stress state of an uncracked half plane. The values of SIF can be obtained using the relative displacements of the crack faces as follows: First the stress values along the line of the crack in its absence are obtained. Then, a distribution of dislocations is introduced along the line of the crack. A dislocation can be formed by cutting out a narrow strip in the half plane and gluing the faces of the cuts together along their entire length.

In the notation of Figure 4 the stress state induced by a dislocation located at (c, 0) whose Burger vector has components (b_x, b_y) [24] is presented as follow:

$$\begin{Bmatrix}\sigma_{xx}\\ \sigma_{yy}\\ \tau_{xy}\end{Bmatrix}=\frac{G}{\pi(\kappa+1)}\left\{\begin{Bmatrix}G_{xxx}(x,y,c)\\ G_{xyy}(x,y,c)\\ G_{xxy}(x,y,c)\end{Bmatrix}b_x+\begin{Bmatrix}G_{yxx}(x,y,c)\\ G_{yyy}(x,y,c)\\ G_{yxy}(x,y,c)\end{Bmatrix}b_y\right\} \quad (6)$$

where the functions G_{ijk} are defined explicitly in Ref. [16]. The crack to be analyzed is depicted in Figure5. By transforming the stress components from the global coordinate to the local coordinate depicted in Figure 5, we can find a new set of functions, which will become the kernels of integral equations, expressed exclusively in the local coordinate set, viz.

$$\begin{Bmatrix}\tau_{\hat{x}\hat{y}}\\ \sigma_{\hat{y}\hat{y}}\end{Bmatrix}=\frac{G}{\pi(\kappa+1)}\left\{\begin{Bmatrix}K_{\hat{x}}^{S}(\hat{x},c)\\ K_{\hat{x}}^{N}(\hat{x},c)\end{Bmatrix}b_{\hat{x}}(c)+\begin{Bmatrix}K_{\hat{y}}^{S}(\hat{x},c)\\ K_{\hat{y}}^{N}(\hat{x},c)\end{Bmatrix}b_{\hat{y}}(c)\right\} \quad (7)$$

Now, if instead of installing a discrete dislocation, we introduce a distribution of dislocations of densities $B_{\hat{x}}(c)$ and $B_{\hat{y}}(c)$ defined by:

$$B_{\hat{i}}=\frac{db_{\hat{i}}(c)}{d\hat{x}} \qquad i=x \text{ or } y \quad (8)$$

We can see that the total normal traction, $N(\hat{x})$, and shear traction, $S(\hat{x})$, across the crack are given by:

$$S(\hat{x})=\tau_T(\hat{x})+\frac{G}{\pi(\kappa+1)}\left\{\int_0^b B_{\hat{x}}(c)K_{\hat{x}}^{S}(x,c)dc+\int_0^b B_{\hat{y}}(c)K_{\hat{y}}^{S}(x,c)dc\right\}$$
$$N(\hat{x})=\sigma_T(\hat{x})+\frac{G}{\pi(\kappa+1)}\left\{\int_0^b B_{\hat{x}}(c)K_{\hat{x}}^{N}(x,c)dc+\int_0^b B_{\hat{y}}(c)K_{\hat{y}}^{N}(x,c)dc\right\} \quad (9)$$

where $\sigma_T(\hat{x})$ and $\tau_T(\hat{x})$ are the values of the tractions induced along the line of the crack by applied loads. One should note that for traction free crack faces we have $N(\hat{x})=S(\hat{x})=0$.

The first step in numerical solution of Eq.9 is to normalize the variables, which can be accomplished by introducing new variables given by:

$$r=2c/b-1, s=2\hat{x}/b-1 \quad (10)$$

By introducing the unknown function of Eq. 9 as:

$$B_{\hat{i}}=\phi_{\hat{i}}\sqrt{\frac{1+r}{1-r}} \qquad i=x \text{ or } y \quad (11)$$

And switching to a series representation such that a system of simultaneous linear algebraic equations remain:

$$\frac{Gb}{2\pi(\kappa+1)}\sum_{i=1}^{n}\frac{2\pi(1+r_i)}{2n+1}\left\{K_{\hat{x}}^{S}(s_k,r_i)\phi_{\hat{x}}(r_i)+K_{\hat{y}}^{S}(s_k,r_i)\phi_{\hat{y}}(r_i)\right\} \quad (12)$$
$$=-\tau_T(s_k)$$
$$\frac{Gb}{2\pi(\kappa+1)}\sum_{i=1}^{n}\frac{2\pi(1+r_i)}{2n+1}\left\{K_{\hat{x}}^{N}(s_k,r_i)\phi_{\hat{x}}(r_i)+K_{\hat{y}}^{N}(s_k,r_i)\phi_{\hat{y}}(r_i)\right\} \quad (13)$$
$$=-\sigma_T(s_k)$$

Eq. 12 and Eq. 13 yield *2n* simultaneous unknowns $\phi_{\hat{x}}(r_i)$, $\phi_{\hat{y}}(r_i)$. Once these values have been found, the SIFs can be deduced from the basic fracture mechanics equations as:

$$K_I=2\sqrt{2}\sqrt{\pi b}\frac{G}{\kappa+1}\phi_{\hat{y}}(1)$$
$$K_{II}=2\sqrt{2}\sqrt{\pi b}\frac{G}{\kappa+1}\phi_{\hat{x}}(1) \quad (14)$$

5. STRAIN ENERGY DENSITY CRITERION

As noted earlier, fretting fatigue cracks generally experience growth on a mixed mode fashion. Thus, having a knowledge on SIFs alone cannot lead to a fine evaluation of crack behavior and one should use a certain criteria developed for this purpose. Characterizing a combination of SIFs in different modes of fracture, these criteria generally are adopted in predicting both the direction of crack growth and the critical applied load under monotonic loadings for mixed mode problems. The strain energy density criterion, also called *S*-criterion, has shown to be very efficient for this purpose [26-29], and is applied in this study. In this criterion, attention is focused on the singularity strength of the strain energy field around the crack tip. This energy filed has a singularity whose strength is designated as the "strain energy density factor", S. The basic assumption in this criterion is that cracks initiate to grow when the interior minimum of the strain energy density factor reaches a critical value [26]. The strain energy density factor *S* is related to the strain energy density function $dW/dV=S/r$ where *r* is the distance from the crack tip. The critical value of dW/dV can be determined from the area under uniaxial stress and strain curve. For the asymptotic analysis *S* depends only on the angle θ. For the plane problems, *S* as a function of θ, can be found as follows [26]:

$$S(\theta)=a_{11}K_1^2+a_{12}K_IK_{II}+a_{22}K_{II}^2 \quad (15)$$

where

$$a_{11}=\frac{1}{16G\pi}[(1+\cos\theta)(\kappa-\cos\theta)]$$
$$a_{12}=\frac{1}{16G\pi}\sin\theta[2\cos\theta-(\kappa-1)]$$
$$a_{22}=\frac{1}{16G\pi}[(1-\cos\theta)(\kappa+1)+(1+\cos\theta)(3\cos\theta-1)] \quad (16)$$

The initial crack growth takes place in the direction

of minimum S, so that:

$$\frac{dS}{d\theta} = 0 \quad \text{at } \theta=\theta_0 \qquad (17)$$

where $-\pi < \theta < \pi$. This criterion also suggests crack initiation occurs when S reaches a critical value S_{cr}, which:

$$S_{cr} = a_{11}K_1^2 + a_{12}K_I K_{II} + a_{22}K_{II}^2 \quad \text{for } \theta=\theta_0 \qquad (18)$$

6. DISCUSSION

Fretting fatigue of a half plane in contact with a flat rounded pad placed under fretting loading is taken into consideration. The SIFs of resulting slant fretting cracks in the first and second modes of fracture are calculated and their cumulative effect on crack growth is investigated using the strain energy density criterion.

The first step in the present study of fretting fatigue is to determine the stress state of the half plane in contact with a flat rounded pad. The specifications of the contact and its loading are given in Table 1. The values of σ_x in the depth of 0.1mm from the half plane surface are shown in Figure 6.

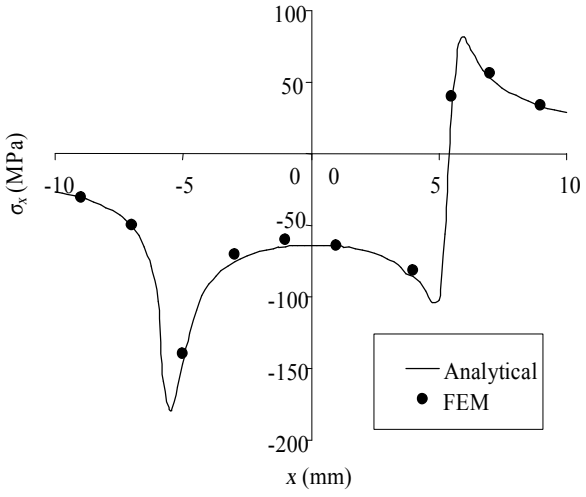

Figure 6. σ_x in the depth of 0.1mm from contact surface

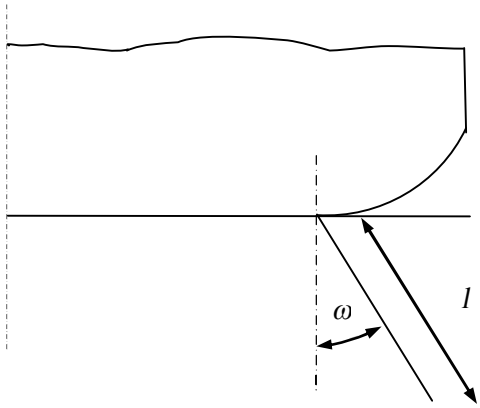

Figure 7. An arbitrarily slant crack at the edge of contact with the length of l and orientation angle

TABLE 1. Flat rounded contact problem specifications

E (MPa)	v	R (mm)	a (mm)	P (N)	Q (N)	σ_b (Mpa)	f
26000	0.3	100	5	896	376	23.68	0.5

Good agreement between the results of described method and FEM can be seen in Figure. 6. A peak value of σ_x can be observed near the contact boundary which may justify rapid crack growth in this zone. The calculated stress state in the half plane and also FEM results show that the contact boundary zone undergoes the maximum tensile stress.

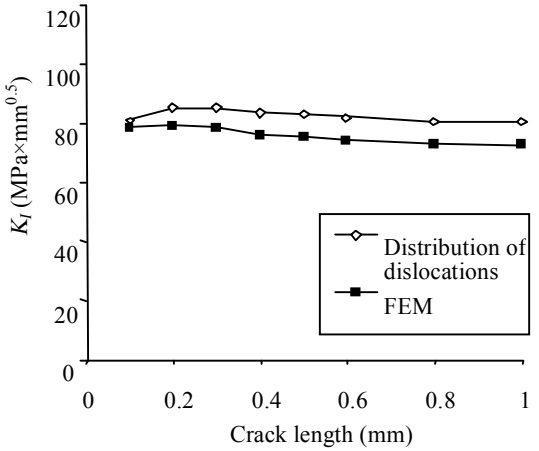

Figure 8. The K_I values of normal fretting cracks in the half plane

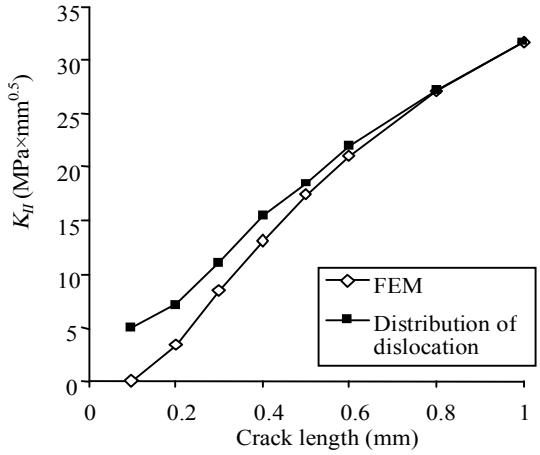

Figure 9. The K_{II} values of normal fretting cracks in the half plane

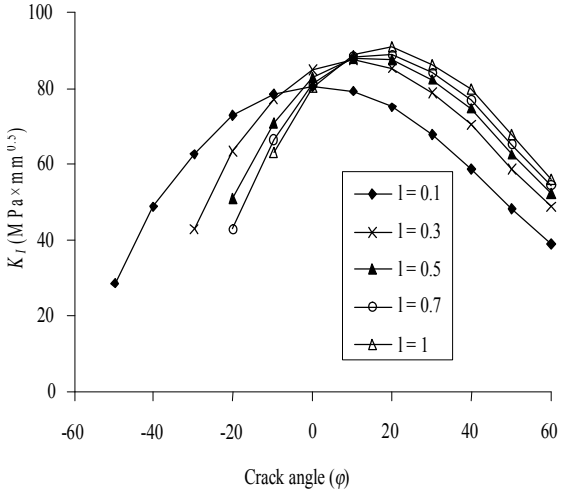

Figure 10. The K_I values of slant cracks with different lengths and inclinations

Experimental studies also show that fretting fatigue cracks tend to appear in this zone [30, 31, 32][30-32]. Therefore, we consider the cracks at x = 5.7mm, where is the contact boundary. Slants cracks with length l (0.1mm $\leq l \leq$ 1mm) and the orientation to surface normal varying over the range $-50<\varphi<60$ are taken into consideration (Figure 7).

The values of K_I and K_{II} are calculated for normal cracks with different lengths using finite element method and compared to the results of distribution of dislocations method (Figure 8 and Figure9). The values of K_I and K_{II} for slant cracks are shown in Figure 10 and Figure 11, respectively. There is a limitation on the calculation of SIFs for cracks with negative values of φ as the crack may be partially closed which is not in the scope of the present study. As shown in Figure 10, for every specific length of the crack, a peak in the K_I values can be found. The orientation of the crack in these peak points depends on the crack length, so that for shorter cracks it is almost zero but it increases for the longer cracks. A quite different pattern can be observed in the variations of K_{II} .

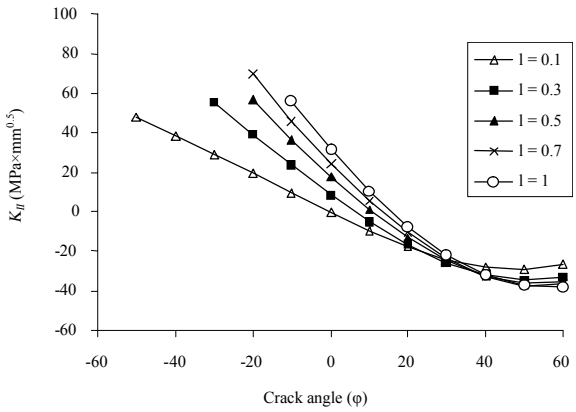

Figure 11. The K_{II} values of slant cracks with different lengths and inclinations

As shown in Figure 11, the lowest absolute values of K_{II} belong to almost normal cracks. A slight orientation of the crack in negative direction causes an abrupt increase in the absolute value of K_{II}. Note that in regard to the K_{II} values, we are more interested in the absolute values rather than their signs. It is because the sign of K_{II} has no intrinsic implication and is utilized in Figure 11 for a deeper conception of its variations with respect to the crack length and orientation.

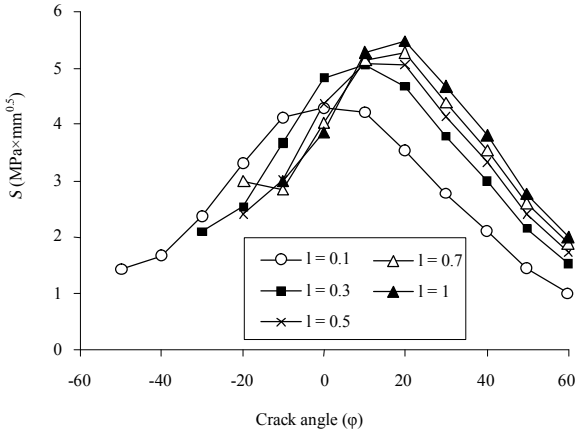

Figure 12. The S values of slant cracks with different lengths and inclinations

Figure 12 shows that any crack longer than 0.1mm exhibited the maximum S values at approximately same angles, whereas this angle decreases sharply when the crack length is reduced to 0.1mm. This is an indication than the crack growth direction is strongly affected by the crack length when the cracks are approximately 0.1mm long. This sensitivity however decreases at longer crack lengths such that beyond 0.1mm crack length, the direction of crack growth is generally unaffected by the crack length.

One may notice that for the normal studied cracks, K_I dominates K_{II} , therefore, scrutinizing the K_I values may well suffices for the evaluation of crack behavior from a fracture mechanics point of view. However, for the case of slant cracks, K_I and K_{II} have analogous values and a convenient criterion for mixed mode fracture should be applied. Using the obtained SIFs for different cracks, we apply the S-criterion in this study specially to evaluate the slant cracks behavior. The strain energy density factors, S, pertinent to the examined cracks are shown in Figure 12. The S value variations have almost the same pattern observed for K_I over a wide range of orientation angles. This conformity attests to the dominant role of K_I on crack growth. For the most negative oriented cracks, K_{II} increases abruptly and affects the S values accordingly. However, this sudden increase in the S values of quite long slant cracks is not a significant concern, because the creation of this form of crack is far from the experimental observations. Thus, it may be concluded that peak values in the calculated Ss show that cracks with the angle of orientation $0^0<\varphi<20^0$ are the most critical ones.

The predictions of the crack growth in the current study were compared with the available experimental observations. Several experimental studies show that the initial growth of fretting cracks is slightly inclined toward the direction of applied bulk stress (direction of applied σ_x in Figure 2), followed by a relatively perpendicular direction to the applied load [14, 16, 32]. The inclination of the cracks toward the applied bulk stress is quite in agreement with the current study, where it was predicted that cracks tend to deviate from perpendicularity up to 20° in the direction of applied bulk stress. It was also expected from the current study that as cracks grow longer, they should follow a perpendicular direction to the bulk stress, where the mode II stress intensity factor becomes negligible, and the mode I stress intensity factor drives the crack growth. The current study however fails to accurately predict the crack trajectory accurately, as it cannot take into account the curved crack path normally observed in the experimental studies.

7. CONCLUSIONS

The growth of slant cracks induced by fretting fatigue of a half plane in contact with a flat rounded pad is studied. The SIFs of resulting slant cracks in the first and second modes of fracture are calculated and their cumulative effect on crack growth is investigated using the strain energy density criterion. The length of studied cracks varies from 0.1 mm to 1 mm and a wide range of orientation angles to surface normal is taken into consideration.

For every examined length of the crack, a peak in the first mode SIFs can be found. The orientation of the crack in these peak points depends on the crack length, so that for shorter cracks it is almost zero but it increases for longer cracks to about 20^0 outward the contact zone for cracks with 1 mm length.

A quite different pattern can be observed in the variations of second mode SIFs, so that their lowest absolute values belong to almost normal cracks. A slight inward orientation of the crack causes an abrupt increase in the absolute value of second mode SIFs.

The variation of strain energy density factor, S, have almost the same pattern observed for the first mode SIFs over a wide range of orientation angles. This conformity attests to the dominant role of first mode of fracture on crack growth. Based on the observation of S versus crack orientation, one may conclude that depending on the crack length, the most critical cracks are those orientated 0^0 to 20^0 outward the contact zone.

Nomenclature

a half of the contact width
b half of the pad flat central part; crack length
$b_i i$ component of the burger vector of a dislocation
B_i density of distribution of dislocations in i direction
c half of the stick zone width
e contact stick zone shift
E modulus of elasticity
f coefficient of friction
g tangential relative slip of contact surface points
G modulus of rigidity
K_I stress intensity factor in mode I
K_{II} stress intensity factor in mode II
M moment created by asymmetrical pressure distribution of the contact area
N total normal traction on crack path
p normal traction on contact area
P normal contact force
Q shear traction on contact area
Q tangential force on pad
r distance from crack tip
R pad corners radius
S strain energy density factor; total shear traction on crack path
S_{cr} critical strain energy density factor
v Poisson's ratio
W strain energy
σ_b bulk stress
σ_T normal traction on crack path due to loading
τ_T shear traction on crack path due to loading

8. REFERENCES

1. Papanikos P, Meguid SA. Theoretical and experimental studies of fretting-initiated fatigue failure of aeroengine compressor discs. ***Fatigue and Fracture of Engineering Materials and Structures***, 17(1994) 539–550.
2. Ciavarella M, Demelio G. A refined CLNA model in fretting fatigue using asymptotic characterization of the contact stress fields, ***International Journal of Solids and Structure***, 38 (2001) 1791–1811.
3. Tang H, Cao D, Yao H, Xie M, Duan R. Fretting fatigue failure of an aero engine turbine blade, ***Engineering Failure Analysis***, 16 (2009) 2004–2008
4. Chan KS, Enright MP, Moody JP, Golden PJ, Chandra R, Pentz AC. Residual stress profiles for mitigating fretting fatigue in gas turbine engine disks. ***International Journal of Fatigue***, 32 (2010) 815–823.
5. Mc Veigh PA, Farris TN. Analysis of surface stresses and stress intensity factors present during fretting fatigue, AIAA -99-1337:1188–1196.
6. Ciavarella M, Macina G. New results for the fretting-induced stress concentration on hertzian and flat rounded contacts. ***International Journal of Mechanical Sciences***, 45 (2003) 449–467.
7. Hutson AL, Nicholas T, Goodman R. Fretting fatigue of Ti-6Al-4V under flat-on-flat contact. ***International Journal of Fatigue***, 21 (1999) 663–669.
8. Dini D, Nowell D. Prediction of the slip zone friction coefficient in flat and rounded contact. ***Wear*** 254 (2003) 364–369.
9. Jin O, Mall S. Influence of contact configuration on fretting fatigue behavior of Ti–6Al–4V under independent pad displacement condition. ***International Journal of Fatigue***, 24 (2002) 1243–1253.
10. Ciavarella M, Demelio G. A review of analytical aspects of fretting fatigue, with extension to damage parameters, and application to dovetail joints. ***International Journal of Solids and Structures***, 38 (2001) 1791–1811.
11. Kim HS, Mall SH. Investigation into three-dimensional effects of finite contact width on fretting fatigue. ***Finite Elements in Analysis and Design***, 41 (2005) 1140–1159.
12. Dini D, Nowell D. Flat and rounded fretting contact problems, incorporating elastic layers. ***International Journal of Mechanical Sciences***, 46 (2004) 1635–1657.
13. Kim HK, Lee SB. Crack initiation and growth behavior of Al2024-T4 under fretting fatigue. ***International Journal of Fatigue***, 19 (1997) 243–51.
14. Naboulsi S, Mall S. Fretting fatigue crack initiation behavior using process volume approach and finite element analysis. ***Tribology International***, 36 (2003) 121–131.
15. Lykins CD, Mall S. Jain VK. A shear stress based parameter for fretting fatigue crack initiation. ***Fatigue and Fracture of Engineering Materials and Structures***, 24 (2001) 461–73.
16. Hills DA, Nowell D. Mechanics of Fretting Fatigue. Kluwer Academic Publishers, Dordrecht, 1994.
17. Jaeger J. New analytical solutions for a flat rounded punch compared with FEM. in Computational methods in contact mechanics V, Eds.: J. Dominguez, C.A. brebbia, WIT Press, Southamption, 2001: 307–316.
18. Erdogan F, Gupta GD. On the numerical solution of singular integral equations. ***Quarterly of Applied Mathematics***. 1972; Jan.: 525–534.
19. Nowell D, Hills DA. Mechanics of fretting fatigue. ***International Journal of Mechanical Science***, 29 (1987) 355–365.
20. Muskhelishvili NI. Singular Integral Equations, Boundary Problems of Function Theory and their Application to mathematical physics. Noordhoff: Groningen, 1953.
21. Hills DA, Nowell D, Sackfield A. Mechanics of Elastic Contacts. Oxford: Butterworth-Heinemann, 1993.
22. Madge JJ, Leen SB, Shipway PH. The critical role of fretting wear in the analysis of fretting fatigue, ***Wear*** 263 (2007) 542–551.
23. Tarafder M, Tarafder S, Ranganath VR, Ghosh RN. Finite element solutions for stress intensity factors in longitudinally cracked cylindrical components. ***International Journal of Pressure Vessels and Piping***, 70 (1997) 127–133.

24. Hills DA, Nowell D. Stress intensity calibrations for closed cracks. ***Journal of Strain Analysis***, 24 (1989):37–43.
25. Bjerkén C, Melin S. Growth of a short fatigue crack – A long term simulation using a dislocation Technique, ***International Journal of Solids and Structures***, 46 (2009) 1196–1204.
26. Sih GC. Prospects of Fracture Mechanics, Noordhoff: Leiden, 1975.
27. Sih GC. Methods of analysis and solutions of crack problems, in mechanics of fracture, Noordhoff: Leiden, 1973.
28. Sih GC. Strain energy density factor applied to mixed mode crack problems. ***International Journal of Fracture***, 10 (1974) 305–321.
29. Xie YJ, Hills DA. Crack Initiation at contact surface. ***Theoretical and Applied Fracture Mechanics***, 40 (2003) 279–283.
30. Waterhouse RB. Fretting Fatigue. London: Applied Science Publishers, 1981.
31. Endo K, Goto H. Initiation and propagation of experimental and theoretical study, ***International Journal of fretting fatigue cracks. Wear***, 38(1976) 311–324.
32. Jacob MSD, Arora PR, Saleem M, Ahmed EM, Sapuan SM. Fretting fatigue crack initiation: ***An Fatigue,*** 29 (2007) 1328–1338.